

The Massive Cosmic Neutrino Background

K. Schutz*

MIT Department of Physics

(Dated: May 7, 2013)

Experimental observations of flavor oscillations prove that neutrinos must have a nonzero rest mass. This is surprising because massive neutrinos are not predicted by the “vanilla” Standard Model of particle physics, and this discrepancy may lead to new physics beyond the Standard Model. Unfortunately, the neutrino mass is still unknown, as it is too small to directly measure in a neutrino detector. However, relic neutrinos from the Big Bang fill our universe, and there are many ways we can use these cosmic neutrinos to measure the neutrino mass. Using quantum statistical mechanics, we derive properties of this neutrino background, including the entropy density, number density, and temperature of the cosmic neutrinos throughout the history of our universe. We also discuss methods for imposing cosmological constraints on the neutrino mass from structure formation, including the current upper bounds from each of those methods.

I. INTRODUCTION

Neutrinos are elementary spin-1/2 fermions, named for their property of electric neutrality, which indicates that they are not affected by the electromagnetic force. Neutrinos are leptons, so they are also unaffected by the strong nuclear force but they do interact via the weak force. In fact, neutrinos interact so weakly that billions stream through us every second without interacting.

Until recent years, it was believed that neutrinos were massless. However, in the past few decades many neutrinos experiments have confirmed that neutrinos oscillate [1–7], a phenomenon that was first predicted in 1957 by Bruno Pontecorvo [8]. Neutrinos come in three flavors corresponding to the other fundamental leptons, namely electron, mu, and tau. Neutrinos have been observed to oscillate between flavors, which means that neutrinos must experience the passage of time in their rest frame. This proves that neutrinos cannot be traveling at the speed of light, so therefore they must have a nonzero mass. The fact that neutrinos oscillate arises from the fact that they propagate in mass eigenstates, but we observe them in flavor eigenstates. Massive neutrinos are not predicted by the “vanilla” Standard Model and this discrepancy may help bridge the gap to human discovery of physics beyond the Standard Model.

The neutrino masses have never been experimentally detected because neutrino oscillation experiments are only sensitive to pairwise differences in the squares of the masses. At least one of the neutrinos in any given pair must have a mass-squared that is greater than the pair’s mass-squared difference (otherwise the other mass-squared would have to be negative.) Based on the greatest mass-squared difference we have observed, we know experimentally that there must be one neutrino mass eigenstate with a mass of at least $0.04 \text{ eV}/c^2$ [9]. This is the only lower bound that we have, and it sets the scale for the neutrino masses. Unfortunately, it is not

currently possible to directly detect such an exceedingly small mass in a neutrino detector; the smallest energies that neutrino detectors can observe is in the range of 10^8 eV , which is nowhere near the scale of 0.04 eV .

Fortunately, the universe itself provides us with a built-in probe of relic neutrinos from the Big Bang, known as the Cosmic Neutrino Background (CNB). Despite the fact that these relic neutrinos fill space, we lack the technology to detect them directly because of the combination of their low temperature (which we calculate in Section V) and the fact that they only interact weakly. However, small neutrino masses have a non-negligible effect on the structural development of the early universe. The ultimate goal of this paper is to showcase some of the many ways we can use cosmic neutrinos to place an upper bound on the neutrino mass, in spite of the fact that we cannot directly detect them.

The paper is organized as follows. In Section II we review the dynamics of our expanding universe. We will then perform a series of calculations in Section III to determine the thermal properties of the relativistic particles in the early universe. In Section IV, we calculate the temperature at which neutrinos come out of equilibrium with the rest of the particles in the early universe, a transition known as *decoupling*. This decoupling marks the emission of the Cosmic Neutrino Background from the neutrinos’ surface of last scattering. In Section V, we calculate the present-day temperature of the resulting cosmic neutrinos, and we find that direct detection is unfeasible due to the low CNB temperature. Finally, in Section VI, we discuss some of the ways that we can overcome this hurdle and constrain the neutrino mass using the gravitational clustering properties of neutrinos.

II. THE EXPANDING UNIVERSE

We live in a universe that is uniform (homogeneous) and the same in all directions (isotropic). This spacetime geometry is described most generally by the Friedmann-Robertson-Walker (FRW) metric. The spacetime of an FRW universe is marked by a scale factor $a(t)$, which gives the conversion between comoving and physical dis-

*Electronic address: kschutz14@mit.edu

tances, which are depicted in Figure 1. More explicitly, the conversion goes like:

$$d_{phys}(t) = a(t)d_c. \quad (1)$$

Not only does the scale factor affect the distance between objects, but it also affects the wavelengths of light. For example, since our universe is expanding, photons from distant sources have their wavelengths increased on their journey to our telescopes since the scale factor has changed over time.

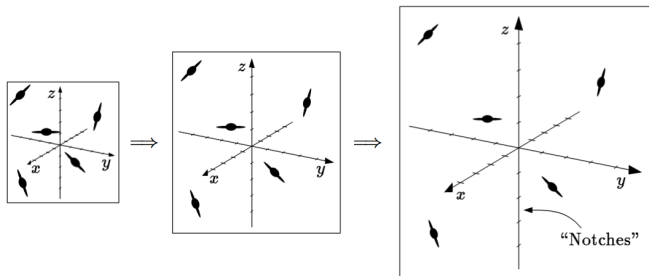


FIG. 1: An illustration of the changing scale factor for an expanding universe. Here “notches” correspond to comoving coordinates. The comoving coordinates are unaffected by the expansion, but the physical distances change by a factor of $a(t)$. Image source: Alan Guth.

The dynamics of the universe are then governed by the Friedmann equation, which is derived by solving the Einstein field equations for a perfect fluid in a homogeneous and isotropic spacetime that is spatially flat [10].¹ The Friedmann equation is:

$$H^2 \equiv \left(\frac{\dot{a}}{a}\right)^2 = \frac{8\pi G_N \rho}{3} \quad (2)$$

where H is known as the Hubble parameter, G_N is Newton’s gravitational constant, and ρ is the energy density of the universe. This equation tells us about the expansion rate of the universe based on how much energy there is driving the expansion.

III. QUANTUM STATISTICAL MECHANICS OF RELATIVISTIC PARTICLES

The early universe was a hot, dense plasma made of elementary particles. At very early times, the types of

particles present was governed by a number of exotic, high-energy phenomena that are not fully understood. However, at relatively late times, approximately 1 second after the big bang, the thermal energy scale of the universe was in a regime where we understand the physics very well. We are concerned with this era in particular because that is the approximate time when neutrinos come out of thermal equilibrium, a process known as *decoupling* that we describe in more detail in Section IV.

Right before the neutrinos decouple, the universe is primarily made up of photons, electron-positron pairs, neutrinos, and the occasional proton or neutron [12]. Before we can understand how the neutrinos decouple we must first derive some basic thermal properties of the early universe. In particular, we seek to derive some basic properties about the entropy, number density, and energy density of relativistic particles. (We do not consider the thermal properties of the protons and neutrons. They are nonrelativistic when the neutrinos decouple, which exponentially suppresses their entropy density etc. [10].)

The statistics of photons in the early universe are governed by the usual Bose-Einstein occupation number [13]:

$$f_{BE} = \frac{1}{e^{(E-\mu)/k_B T} - 1}. \quad (3)$$

Meanwhile, neutrinos and electrons are fermions, which means that the occupation number follows Fermi-Dirac statistics [13]:

$$f_{FD} = \frac{1}{e^{(E-\mu)/k_B T} + 1}. \quad (4)$$

We define E to be the energy of the particles, given by the usual relativistic energy formula $E(p) = \sqrt{p^2 c^2 + m^2 c^4}$. We also define μ to be the chemical potential, k_B to be the Boltzmann constant, and T the temperature. The photon chemical potential is zero because the number of photons is not generally conserved. Meanwhile, for the purposes of our calculations, we set the neutrino chemical potential μ_ν to zero. This is a reasonable assumption because conservation of lepton number requires that the chemical potential be entirely negligible during Big Bang Nucleosynthesis (BBN) [12].²

The energy density ρ is given by the integral of energy over phase space and weighted by the occupation number. Here the phase space volume for a given state in three dimensions will be $(2\pi\hbar)^3$ due to the uncertainty principle, so the density of states for a three-dimensional particle is given by $d^3x d^3p / (2\pi\hbar)^3$ [14]. Therefore, the total energy density [13] of any given type of particles will be

$$\rho = g \int \frac{d^3p}{(2\pi\hbar)^3} \frac{E(p)}{e^{E(p)/k_B T} \pm 1} \quad (5)$$

¹ For the purposes of this paper, we assume that we can neglect any global curvature and that we live in a spatially flat universe. This constraint is well-motivated by measurements of the universe that indicate flatness. In order for the universe to be anywhere near flat at present-times, curvature had to be extremely suppressed at early times. See [11] for an in-depth discussion.

² Using a nonzero neutrino chemical potential only increases the total energy density and therefore shortens the time scale of decoupling. See [12].

where g is the degeneracy of that particle. Meanwhile, the pressure, P of a system [13] is given by:

$$P = g \int \frac{d^3p}{(2\pi\hbar)^3} \frac{p^2}{3E(p)(e^{E(p)/k_B T} \pm 1)}. \quad (6)$$

One form of the first law of thermodynamics allows us to derive the entropy density $s(T)$ as follows:

$$\begin{aligned} d(s(T)V) &= \frac{d(\rho(T)V) + P(T)dV}{T} \\ \Rightarrow s(T) &= \frac{\rho(T) + P(T)}{T}. \end{aligned} \quad (7)$$

As previously mentioned, nonrelativistic particles have negligible entropy density in the early universe. For the ultrarelativistic particles, $E(p) \approx pc$ and if we combine Equations (5) and (6), we see that the entropy density will be $s = 4\rho/3T$, which gives us

$$s = \frac{4g}{3T} \int \frac{d^3p}{(2\pi\hbar)^3} \frac{pc}{e^{pc/k_B T} \pm 1}. \quad (8)$$

We can evaluate this integral by switching to polar coordinates and using a substitution $x \equiv pc/k_B T$, so we now get:

$$s = \frac{16\pi g k_B^4 T^3}{(2\pi\hbar)^3 c^3} \int \frac{x^3 dx}{e^x \pm 1}. \quad (9)$$

When we evaluate this integral, we get:

$$s = \begin{cases} \frac{7}{8} g \left(\frac{2\pi^2 k_B^4 T^3}{45 (\hbar c)^3} \right) & \text{for fermions} \\ g \left(\frac{2\pi^2 k_B^4 T^3}{45 (\hbar c)^3} \right) & \text{for bosons} \end{cases} \quad (10)$$

Similarly, to calculate the number density, $n(T)$ of particles [13] in the early universe, we integrate the occupation number over phase space:

$$n = g \int \frac{d^3p}{(2\pi\hbar)^3} \frac{1}{e^{E(p)/k_B T} \pm 1}. \quad (11)$$

Again, we find that if we switch to polar coordinates and make the substitution $x \equiv pc/k_B T$, we are left with this integral:

$$n = \frac{g(k_B T)^3}{2\pi^2 (\hbar c)^3} \int \frac{x^2 dx}{e^x \pm 1} \quad (12)$$

and ultimately, we find:

$$n = \begin{cases} \frac{3}{4} g \left(\frac{\zeta(3)(k_B T)^3}{\pi^2 (\hbar c)^3} \right) & \text{for fermions} \\ g \left(\frac{\zeta(3)(k_B T)^3}{\pi^2 (\hbar c)^3} \right) & \text{for bosons} \end{cases} \quad (13)$$

where ζ is the the Riemann zeta function.

We calculate the particle degeneracy, g , by simply counting the number of ways of having a given type of

particle in the distribution. The general prescription for calculating the particle degeneracy is the following:

$$\begin{aligned} g &= \text{number of flavors} \times \text{number of spin states} \\ &\times 2 \text{ for particle/antiparticle pair degeneracy} \end{aligned} \quad (14)$$

So $g_\gamma = 2$ because there are two photon polarizations and photons do not have an antiparticle. Next, $g_{e^-} = 4$ since electrons and positrons each have two spin orientations because they are spin 1/2 particles. Finally, $g_\nu = 6$ because neutrinos and antineutrinos come in three degenerate flavors in the early universe: electron, mu, and tau. Interestingly, despite the fact that neutrinos are spin 1/2 fermions, the only neutrinos that are found in nature have left-handed spin polarization, and therefore there is only one spin degree of freedom for neutrinos. The theoretical basis for this oddity is a point of contention depending on which model one subscribes to, and we will not discuss it further here.

IV. SCATTERING AND DECOUPLING

In the early universe, primordial neutrinos were in thermal equilibrium with a hot plasma of electrons, positrons, photons, and the occasional proton or neutron. They maintained thermal equilibrium by means of scattering. This may seem surprising, since neutrinos interact so weakly that billions stream through us every second without scattering. However, early universe neutrinos stayed in thermal equilibrium with the rest of the particles because the early universe was incredibly dense. Additionally, the weak scattering cross section of the neutrino is dependent on temperature, and the early universe was quite hot. Weak scattering is mediated by the W boson, which is a force carrier particle with a rest energy of 80 GeV. When the temperature falls below the rest energy of the W boson, which still corresponds to a very high temperature, the neutrino cross section for neutrino-electron scattering [12] is:

$$\sigma_{wk} = \left(\frac{G_F}{(\hbar c)^2} k_B T \right)^2 \quad (15)$$

where G_F is the weak interaction coupling constant, which according to NIST has a value of $G_F/(\hbar c)^3 = 1.17 \times 10^{-5} \text{ GeV}^{-2}$. In the previous section, we calculated the number density of electrons and neutrinos using Equation (13). Therefore, the weak scattering rate between neutrinos and electrons goes like:

$$\Gamma_\nu = n_e \sigma_{wk} c = \frac{3g\zeta(3)G_F^2 (k_B T)^5}{4\pi^2 \hbar^7 c^6} \quad (16)$$

where we have assumed that the velocity of the scattered particles is ultrarelativistic.

Meanwhile, we can use Equations (2) and (5) to calculate the expansion rate:

$$H = \sqrt{\frac{43\pi^3 G_N (k_B T)^4}{45 (\hbar c)^3}}. \quad (17)$$

The ratio of the collision rate to the expansion rate is then

$$\frac{\Gamma_\nu}{H} = \frac{G_F^2 (k_B T)^3}{4\pi^2 \hbar^7 c^6} \sqrt{\frac{45(\hbar c)^3}{43\pi^3 G_N}} \approx \left(\frac{T}{1 \times 10^{10} \text{ K}} \right)^3. \quad (18)$$

Therefore, once the temperature drops below approximately 10^{10} K, the scattering rate cannot keep up with the expansion rate, and the neutrinos fall out of thermal equilibrium with the rest of the plasma! This is known as *decoupling*, and it signifies the emission of the cosmic neutrino background radiation.

It is of particular interest to note that the decoupling temperature is greater than $m_e c^2 / k_B = 5.9 \times 10^9$ K, the rest energy of the electron positron pairs. At the neutrino decoupling temperature, electron-positron annihilation is just as favorable as pair production. However, after the neutrinos decouple and the temperature drops to below $m_e c^2 / k_B$, the electrons and positrons annihilate because the temperature of the universe no longer has enough energy to support the electron-positron pairs. The annihilation does not affect the neutrinos, which have already come out of thermal equilibrium. The excess energy does, however, heat the photons which are still scattering and maintaining thermal equilibrium with the rest of the primordial plasma. This will play a large role in our determination of the present-day neutrino temperature in the following section.

V. THERMAL PROPERTIES OF THE COSMIC NEUTRINO BACKGROUND

The universe expands adiabatically, which means that the entropy is conserved. In particular, the total entropy in a given physical volume, $s(T)V_{phys} = s(T)a^3 V_C$ must be constant. Therefore, aT must be constant for all times, since $s(T) \sim T^3$ for both fermions and photons. This is a powerful condition that allows us to calculate the neutrino temperature relative to the photon temperature after the electron-positron pairs annihilate.

When all the particles are at the same temperature (before the electron-positron pairs annihilate) the entropy density is given by:

$$s_i = \frac{2\pi^2}{45} \frac{k_B^4 T^3}{(\hbar c)^3} \left[g_\gamma + \frac{7}{8} (g_{e^+e^-} + g_\nu) \right], \quad (19)$$

where T is the common temperature of all the particles and the factor of $7/8$ comes from integrating the Fermi-Dirac distribution, as in Equation (10). As previously mentioned, when the electron-positron pairs annihilate, they only heat the photons and not the neutrinos, which have already come out of thermal equilibrium. Therefore, after the annihilation we must distinguish between the photon temperature and the neutrino temperature:

$$s_f = \frac{2\pi^2}{45} \frac{k_B^4}{(\hbar c)^3} \left(g_\gamma T_\gamma^3 + \frac{7}{8} g_\nu T_\nu^3 \right) \quad (20)$$

where T_ν corresponds to the unchanged neutrino temperature, which is the same as the collective temperature prior to the annihilation.

When we equate the entropy of the universe at times before electron-positron annihilation (19) and afterwards (20), we find the ratio of the neutrino temperature to the photon temperature to be:

$$\frac{T_\nu}{T_\gamma} = \left(\frac{4}{11} \right)^{1/3}. \quad (21)$$

We can therefore directly compare the CNB with the Cosmic Microwave Background (CMB). The CMB is a background of photons that decouples a long time after the neutrinos decouple. Since photons are much easier to detect than neutrinos, we have extensively probed the CMB. Noting the fact that the present day temperature of CMB photons is 2.73 K [15], we find that the cosmic neutrino temperature is 1.95 K.

We can also use this information to determine the ratio of neutrino energy density to photon energy density, as well as the ratio of number densities. In particular,

$$\frac{\rho_\nu}{\rho_\gamma} = \frac{7g_\nu}{8g_\gamma} \left(\frac{4}{11} \right)^{4/3} = \frac{21}{8} \left(\frac{4}{11} \right)^{4/3} \quad (22)$$

$$\frac{n_\nu}{n_\gamma} = \frac{3g_\nu}{4g_\gamma} \left(\frac{4}{11} \right) = \frac{9}{11} \quad (23)$$

Given that a 2.73 K blackbody of photons has an energy density of 0.26 MeV/m³, the cosmic neutrino background will have a present-day energy density of 0.18 MeV/m³. And given that the number density of a 2.73 K blackbody of photons has a number density of 4.1×10^8 /m³, the cosmic neutrino background will have a present-day number density of 3.4×10^8 /m³. Therefore, we calculate the average present-day energy of a cosmic neutrino to be 5.4×10^{-4} eV.

Before proceeding, it is important to note that the neutrino energy we just calculated is inconsistent with our lower bound on the neutrino mass: neutrino oscillation experiments have a lower bound of 0.04 eV for the rest energy of at least one neutrino, which is much larger than 5.4×10^{-4} eV. This inconsistency arose because it was not valid for us to treat the neutrinos as if they were relativistic at late times. In reality, the neutrinos cool as the universe expands since aT is constant. As the neutrinos cool, they become nonrelativistic, with this transition occurring when $k_B T_\nu \sim m_\nu c^2$, which corresponds to a time much earlier than present times. Nonrelativistic neutrinos have an energy density that goes like $\rho_\nu \sim n_\nu m_\nu c^2$, and the transition from neutrinos having relativistic energy to having just their rest energy will play an important role in Section VI, where we examine neutrinos' clustering properties at various points in the history of the universe. In the mean time, it is critical to point out that even though we made an incorrect assumption about neutrinos being relativistic at late times, we were still correct

about the entropy and number densities, as well as the present-day temperature. These vary with expansion the same way whether the neutrinos are relativistic or nonrelativistic; intuitively, the speed of the neutrinos should not change their entropy or number density, which are features of the neutrino radiation associated with conserved quantities. Since the entropy density is unchanged, our assumption that aT is constant is still valid, so the neutrino temperature scales the same way regardless of how fast the neutrinos are moving. Therefore, we still conclude that there is a background of neutrinos with an effective temperature of 1.95 K and a present-day number density of $3.4 \times 10^8 / \text{m}^3$.

Whether or not we assume the neutrinos are relativistic at late times, the cosmic neutrino energy is still far too low to measure in our detectors. The lowest energy neutrinos that neutrino experiments like MicroBooNE and LSND can detect is 200 MeV [16, 17]. The neutrino rest energy is many orders of magnitude below 200 MeV. Therefore, we are nowhere near being able to detect cosmic neutrinos because of how cold they are and how weakly they interact. However, there are other clever ways of utilizing the cosmic neutrino background to probe neutrino physics. In particular, we can see the effects of a background of massive neutrinos on structure formation in the early universe, and we elaborate more in the next section.

VI. CONSTRAINING THE NEUTRINO MASS USING COSMOLOGY

The nonzero neutrino rest mass has a significant effect on how much structure we see on different scales. In particular, massive neutrinos cannot cluster as well on small scales, because small mass overdensities (regions where the mass density is greater than the average) have an escape velocity that is much smaller than the typical neutrino velocity. Therefore a nonzero neutrino mass suppresses smaller-scale structure formation as compared to models where the neutrino mass is zero [18]. We can see signatures of this fact in various types of cosmological probes that correspond to different parts of the universe's evolution. We can combine these measurements to place an upper bound on the sum of the neutrino masses.

One main method of probing the matter distribution involves mapping out visible indicators of mass overdensities. In particular, we can use the CMB as well as the distribution of galaxy clusters, galaxies and neutral hydrogen to create a *power spectrum*. In essence, the power spectrum is just a map of density fluctuations which is then Fourier-transformed and squared. Another useful method of probing the matter distribution involves using *gravitational lensing*, which is the lensing of light due to the curvature of spacetime from foreground mass in the line-of-sight direction. We can use lensing to constrain how much of the foreground mass comes from neutrinos. In the following subsections, we very briefly discuss several of these methods. More in-depth discussion can be found in [19–24].

A. The Cosmic Microwave Background

The CMB power spectrum has been well-probed over the last decade by the WMAP and Planck satellites. The upper bound on the sum of the neutrino masses from the CMB alone is $0.28 \text{ eV}/c^2$ [25, 26]. An additional way

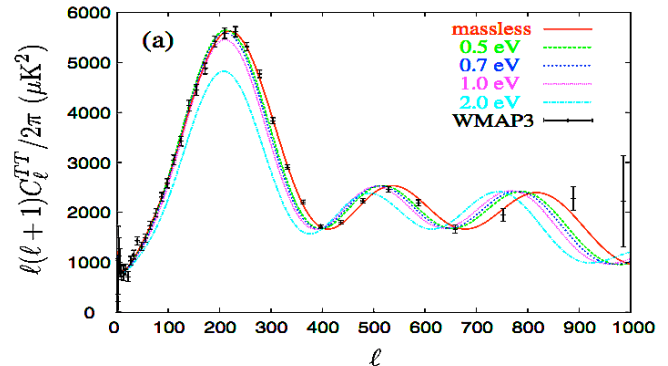


FIG. 2: The angular power spectrum of the CMB from the WMAP 3-year data. This is the decomposition of the Fourier transform of density fluctuations into spherical harmonics. Low l corresponds to large structure, while high l corresponds to smaller-scale structures. This plot also has the predictions that come from adding massive neutrinos to the Standard Model. We can see that more massive neutrinos cause suppression of structure and a shift in the peaks, which indicates that the characteristic size of structure is larger. This plot was reproduced from [27].

to extract information from the CMB comes from measuring its polarization on small scales, which is a good metric of large-scale structure that lenses the CMB in the foreground. Due to the high redshift of the CMB, such lensing measurements probe structure in the early universe, when neutrinos were more relativistic than at late times, making their effect on structures even more dramatic. There currently is no upper bound on neutrino masses from CMB lensing, but experiments like CMBPol have a forecast sensitivity of $\Delta \sum m_\nu = 0.05 \text{ eV}/c^2$ [19].

B. 21 cm Surveys

After the emission of the CMB, the universe was filled with neutral hydrogen gas for millions of years. Neutral hydrogen undergoes a 21 cm hyperfine flip-transition due to the spin-spin interaction between the proton and the electron. If we can detect the 21 cm radiation (which is relatively faint and contaminated by foreground radiation) we can map out the overdensities. Additionally, we can see how redshifted the 21 cm signal is, and therefore we can see how long ago the 21 cm photons were emitted, since the redshift comes from the cosmic expansion over time. So unlike the CMB, which corresponds to a 2-dimensional surface of last scattering, 21 cm surveys actually probe a 3-dimensional volume (two spatial dimensions and one time dimension). Because 21 cm sur-

veys probe a large 3-D volume, there are more samples of any given Fourier mode than in any other cosmological probe that we know of [28]. Therefore, there is an incredible wealth of data to be had from 21 cm surveys, and a 21 cm power spectrum would exquisitely constrain the neutrino mass because of the sheer amount of potential data. We have yet to measure the cosmological 21 cm signal, but there are several experiments underway trying to detect it, such as PAPER, MWA, LOFAR and the Omniscope [29–32]. The most optimistic forecast on the error in the neutrino mass measurement from 21 cm is $\Delta \sum m_\nu = 0.007 \text{ eV}/c^2$ [34].

C. Galaxy Surveys

Galaxy surveys are another way of mapping overdensities. The Sloan Digital Sky Survey (SDSS) [33] has been the largest experiment yet, and it has contributed to the power spectrum at smaller scales much more effectively than CMB experiments (see Figure 3.) We can also use gravitational lensing of galaxies to measure how their images get smeared and distorted, which tells us about clustering in the foreground. Such galaxy survey measurements have constrained the sum of the neutrino masses to be less than $0.6 \text{ eV}/c^2$ [19].

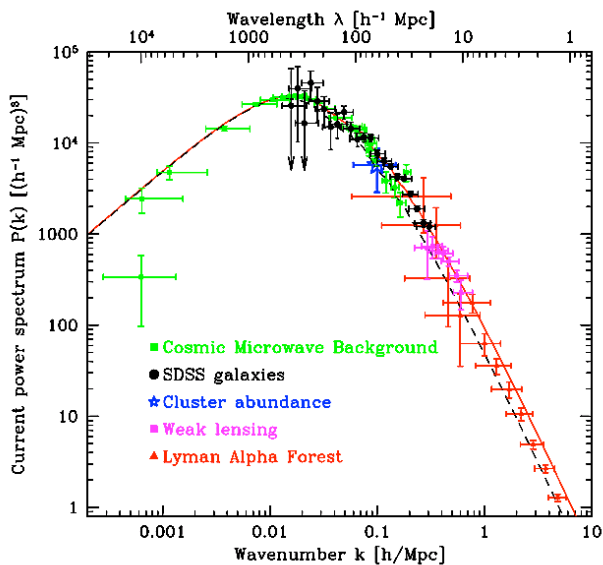


FIG. 3: This is the matter power spectrum at small scales, including data from WMAP, SDSS, lensing, and the Lyman-alpha forest. The solid line marks the theoretical predictions of the Standard Model, whereas the dotted line shows the modification of replacing 7% of the matter with neutrinos with a combined mass of 1 eV. This graph shows that the addition of these massive neutrinos suppresses power on the small scales by about factor of two. This plot was reproduced from [18].

D. Galaxy Clusters

Additionally, we can use galaxy clusters, which are the largest gravitationally bound objects in our universe. Their number in a given volume is drastically affected by the presence of massive neutrinos, which can suppress their formation. The main way we detect clusters is via the *Sunyaev-Zeldovich effect*. This effect causes the heating up of CMB photons due to inverse Compton scattering: low energy photons scatter off of relativistic electrons in the ultradense clusters and thereby gain energy. The upper bound on the sum of the neutrino masses from galaxy clusters is $0.3 \text{ eV}/c^2$ [19].

E. The Lyman-alpha Forest

Finally, we can probe the neutral hydrogen between galaxies using the *Lyman-alpha* series of hydrogen, which corresponds to transitions from the $n = 2$ state to the $n = 1$ state. When we look at distant *quasars*, which are extremely luminous active galactic nuclei, we see a series of absorption lines due to Lyman-alpha transitions in intergalactic hydrogen clouds in our line of sight. The distance between the hydrogen clouds and the quasars determines how much the universe expands between emission by the quasars and absorption by the clouds. Therefore, these Lyman-alpha transitions get redshifted to various extents due to the expansion of the universe at the various different times of absorption. Since the photons pass through a series of clouds, we see a complicated spectrum, which is known as the *Lyman-alpha forest*. The Lyman-alpha forest allows us to use the hydrogen clouds to map out small-scale clustering between galaxies, and therefore the forest indirectly probes the presence of massive neutrinos. The most aggressive upper bound on neutrino masses from the Lyman-alpha forest is approximately $0.17 \text{ eV}/c^2$ [19]. When we combine the constraints from all the effects in the following subsection, we use the more conservative Lyman-alpha upper bound of $0.5 \text{ eV}/c^2$ [18].

F. Neutrino Mass Upper Bound

When we synthesize all of these effects and take into account the associated errors, the constraint on the neutrino masses tightens considerably and the most conservative upper bound on the sum of the neutrino masses is approximately $\sum m_\nu = 0.23 \text{ eV}/c^2$ [26]. This constraint is far better than anything we have from particle detectors, and it is projected to get much better. All of these methods will see their constraints improve with more data from newer experiments, and the most optimistic error forecast is $\Delta \sum m_\nu = 0.007 \text{ eV}/c^2$, which comes from 21 cm experiments [34].

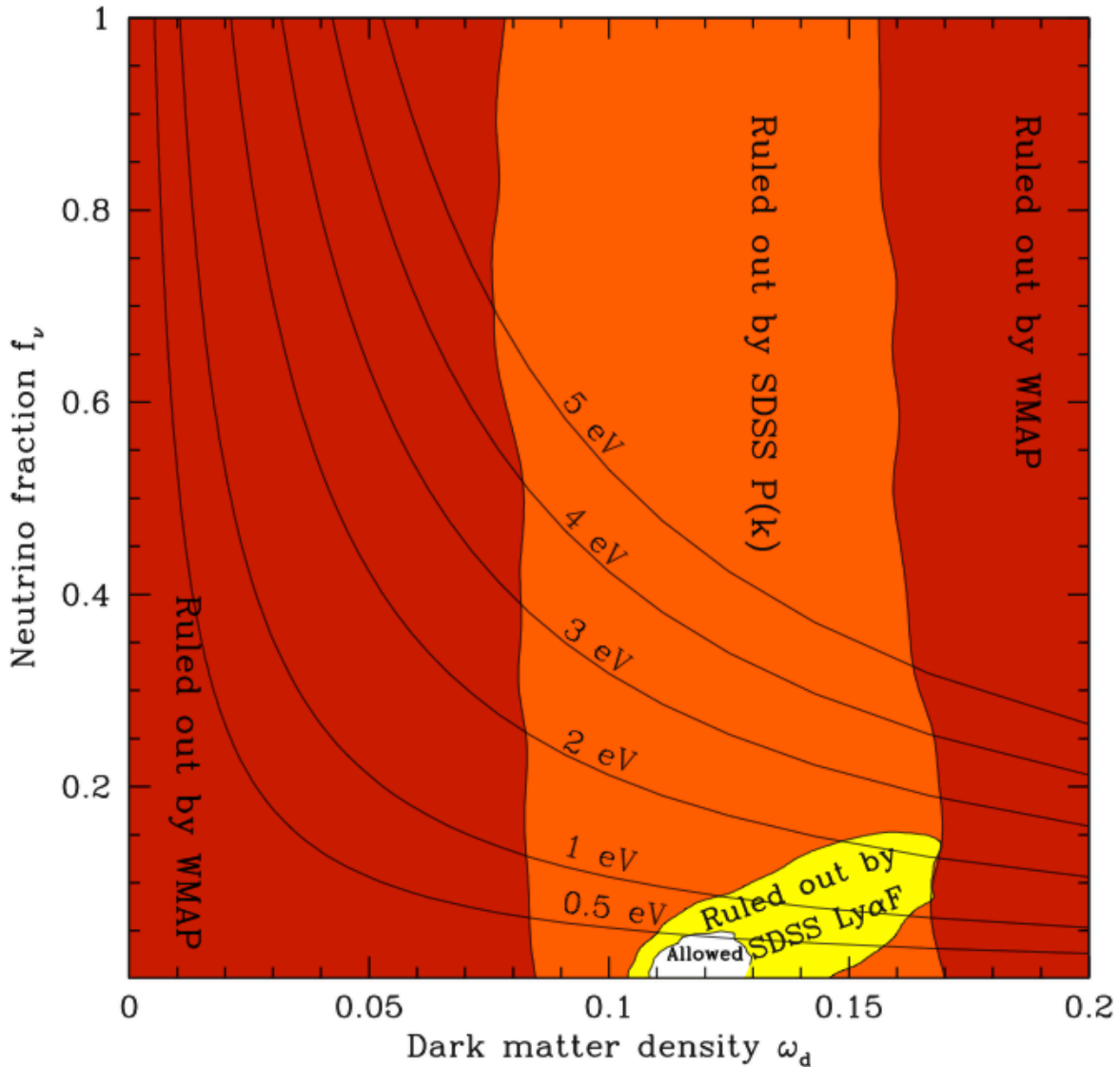


FIG. 4: If we combine several different methods of constraining the neutrino mass, we can rule out huge swatches of parameter space. Here ω_d is the density of dark matter and f_ν is the fraction of the mass density that is made up of neutrinos. The black curves represent different neutrino mass sums. The most conservative bounds from WMAP, SDSS, and the Lyman-alpha forest constrain the sum of the neutrino masses to be less than approximately $0.5 \text{ eV}/c^2$ [18]. If we include the most recent data from the Planck satellite, the conservative upper bound goes to $0.23 \text{ eV}/c^2$ [26]. This plot was reproduced from [18].

VII. CONCLUSION

We have derived several basic properties of the cosmic neutrino background. In particular, we have used quantum statistical mechanics and knowledge of the neutrino scattering cross section to derive the temperature, entropy density, energy density, and number density of this radiation. In light of the fact that neutrinos have mass, we have discussed several methods of utilizing indirect effects of the cosmic neutrino background to constrain the neutrino mass. This remains an exciting and active area of research, with several experiments underway.

Acknowledgments

The author is grateful to Ravi Charan, Daniele Bertolini, Emily Nardoni, and Rudy Tannin for their comments and peer review. Additionally, the author wishes to acknowledge Professor Jesse Thaler, Professor Max Tegmark, and Dr. Mohammad Maghrebi for useful suggestions. Finally, the author is grateful to Adrian Liu for numerous useful conversations pertaining to this work, as well as for his continued support and encouragement.

-
- [1] Y. Fukuda, T. Hayakawa, E. Ichihara, K. Inoue, K. Ishihara, H. Ishino, Y. Itow, T. Kajita, J. Kameda, S. Kasuga, et al., *Physical Review Letters* **81**, 1562 (1998), arXiv:hep-ex/9807003.
- [2] Q. R. Ahmad, R. C. Allen, T. C. Andersen, J. D. Anglin, G. Bühler, J. C. Barton, E. W. Beier, M. Bercovitch, J. Bigu, S. Biller, et al., *Physical Review Letters* **87**, 071301 (2001), arXiv:nucl-ex/0106015.
- [3] T. Araki, K. Eguchi, S. Enomoto, K. Furuno, K. Ichimura, H. Ikeda, K. Inoue, K. Ishihara, T. Iwamoto, T. Kawashima, et al., *Physical Review Letters* **94**, 081801 (2005), arXiv:hep-ex/0406035.
- [4] GALLEX Collaboration, W. Hampel, J. Handt, G. Heusser, J. Kiko, T. Kirsten, M. Laubenstein, E. Pernicka, W. Rau, M. Wojcik, et al., *Physics Letters B* **447**, 127 (1999).
- [5] J. N. Abdurashitov, V. N. Gavrin, S. V. Girin, V. V. Gorbachev, T. V. Ibragimova, A. V. Kalikhov, N. G. Khairnasov, T. V. Knodel, I. N. Mirmov, A. A. Shikhin, et al., *Phys. Rev. C* **60**, 055801 (1999), arXiv:astro-ph/9907113.
- [6] W. W. M. Allison, G. J. Alner, D. S. Ayres, G. Barr, W. L. Barrett, C. Bode, P. M. Border, C. B. Brooks, J. H. Cobb, R. J. Cotton, et al., *Physics Letters B* **449**, 137 (1999), arXiv:hep-ex/9901024.
- [7] MACRO Collaboration, M. Ambrosio, R. Antolini, G. Auriemma, D. Bakari, A. Baldini, G. C. Barbarino, B. C. Barish, G. Battistoni, Y. Becherini, et al., *Physics Letters B* **517**, 59 (2001), arXiv:hep-ex/0106049.
- [8] B. Pontecorvo, *Soviet Journal of Experimental and Theoretical Physics* **6**, 429 (1958).
- [9] Particle Data Group, C. Amsler, M. Doser, M. Antonelli, D. M. Asner, K. S. Babu, H. Baer, H. R. Band, R. M. Barnett, E. Bergren, et al., *Physics Letters B* **667**, 1 (2008).
- [10] S. Dodelson, *Modern Cosmology* (Academic Press, San Diego, 2003).
- [11] A. Guth, *The Inflationary Universe* (Basic Books, New York, 1998).
- [12] S. Weinberg, *Cosmology* (Oxford University Press, 2008).
- [13] R. Baierlein, *Thermal Physics* (Cambridge University Press, 1999).
- [14] D. Griffiths, *Introduction to Quantum Mechanics* (Pearson Prentice Hall, 1995).
- [15] D. J. Fixsen, *Astrophys. J.* **707**, 916 (2009), 0911.1955.
- [16] C. Athanassopoulos, L. B. Auerbach, R. L. Burman, I. Cohen, D. O. Caldwell, B. D. Dieterle, J. B. Donahue, A. M. Eisner, A. Fazely, F. J. Federspiel, et al., *Physical Review Letters* **77**, 3082 (1996), arXiv:nucl-ex/9605003.
- [17] M. Soderberg, in *American Institute of Physics Conference Series*, edited by F. Sanchez, M. Sorel, and L. Alvarez-Ruso (2009), vol. 1189 of *American Institute of Physics Conference Series*, pp. 83–87, 0910.3497.
- [18] M. Tegmark, *Physica Scripta Volume T* **121**, 153 (2005), arXiv:hep-ph/0503257.
- [19] K. N. Abazajian, E. Calabrese, A. Cooray, F. de Bernardis, S. Dodelson, A. Friedland, G. M. Fuller, S. Hannestad, B. G. Keating, E. V. Linder, et al., *Astroparticle Physics* **35**, 177 (2011), 1103.5083.
- [20] A. Dolgov, *Surveys in High Energy Physics* **17**, 91 (2002).
- [21] S. Hannestad, *Annual Review of Nuclear and Particle Science* **56**, 137 (2006), arXiv:hep-ph/0602058.
- [22] G. G. Raffelt, arXiv preprint hep-ph/0208024 (2002).
- [23] J. Lesgourgues and S. Pastor, *Physics Reports* **429**, 307 (2006), arXiv:astro-ph/0603494.
- [24] Y. Y. Y. Wong, *Annual Review of Nuclear and Particle Science* **61**, 69 (2011), 1111.1436.
- [25] E. Komatsu, K. M. Smith, J. Dunkley, C. L. Bennett, B. Gold, G. Hinshaw, N. Jarosik, D. Larson, M. R. Nolte, L. Page, et al., *Astrophys. J. Supplement* **192**, 18 (2011), 1001.4538.
- [26] Planck Collaboration, P. A. R. Ade, N. Aghanim, C. Armitage-Caplan, M. Arnaud, M. Ashdown, F. Atrio-Barandela, J. Aumont, C. Baccigalupi, A. J. Banday, et al., ArXiv e-prints (2013), 1303.5076.
- [27] A. D. Dolgov, *Physics of Atomic Nuclei* **71**, 2152 (2008), 0803.3887.
- [28] M. Tegmark and M. Zaldarriaga, *Phys. Rev. D* **79**, 083530 (2009), 0805.4414.
- [29] A. R. Parsons, A. Liu, J. E. Aguirre, Z. S. Ali, R. F. Bradley, C. L. Carilli, D. R. DeBoer, M. R. Dexter, N. E. Gugliucci, D. C. Jacobs, et al., ArXiv e-prints (2013), 1304.4991.
- [30] S. J. Tingay, R. Goetze, J. D. Bowman, D. Emrich, S. M. Ord, D. A. Mitchell, M. F. Morales, T. Booler, B. Crosse, R. B. Wayth, et al., *PASA* **30**, e007 (2013), 1206.6945.
- [31] V. Kondratiev, B. Stappers, and LOFAR Pulsar Working Group, in *IAU Symposium* (2013), vol. 291 of *IAU Symposium*, pp. 47–52, 1210.7005.
- [32] M. Tegmark and M. Zaldarriaga, *Phys. Rev. D* **82**, 103501 (2010), 0909.0001.
- [33] M. Tegmark, M. A. Strauss, M. R. Blanton, K. Abazajian, S. Dodelson, H. Sandvik, X. Wang, D. H. Weinberg, I. Zehavi, N. A. Bahcall, et al., *Phys. Rev. D* **69**, 103501 (2004), arXiv:astro-ph/0310723.
- [34] Y. Mao, M. Tegmark, M. McQuinn, M. Zaldarriaga, and O. Zahn, *Phys. Rev. D* **78**, 023529 (2008), 0802.1710.